Gas jet disruption mitigation studies on Alcator C-Mod and DIII-D

Citation: R.S. Granetz et al 2007 Nucl. Fusion 47 1086 doi: 10.1088/0029-5515/47/9/003 © IOP Publishing 2007

As Published: http://dx.doi.org/10.1088/0029-5515/47/9/003

Publisher: Institute of Physics Publishing

Persistent URL: http://hdl.handle.net/1721.1/55962

Version: Author's final manuscript: final author's manuscript post peer review, without publisher's formatting or copy editing

Gas Jet Disruption Mitigation Studies on Alcator C-Mod and DIII-D

R.S. Granetz[1], E.M. Hollmann[2], D.G. Whyte[3], V.A. Izzo[1], G.Y. Antar[2], A. Bader[1], M. Bakhtiari[3], T. Biewer[1], J.A. Boedo[2], T.E. Evans[4], I.H. Hutchinson[1], T.C. Jernigan[5], D.S. Gray[2], M. Groth[6], D.A. Humphreys[4], C.J. Lasnier[6], R.A. Moyer[2], P.B. Parks[4], M.L. Reinke[1], D.L. Rudakov[2], E.J. Strait[4], J.L. Terry[1], J. Wesley[4], W.P. West[4], G. Wurden[7], J. Yu[2]

[1] MIT Plasma Science and Fusion Center, Cambridge, MA 02139, US
[2] University of California–San Diego, La Jolla, CA 92093, US
[3] University of Wisconsin–Madison, Dept of Engineering Physics, Madison, WI 53706, US
[4] General Atomics, San Diego, CA 92186, US
[5] Oak Ridge National Laboratory, Oak Ridge, TN 37831, US
[6] Lawrence Livermore National Laboratory, Livermore, CA 94550, US
[7] Los Alamos National Laboratory, Los Alamos, NM 87545, US

E-mail: granetz@mit.edu, ehollmann@ucsd.edu

Abstract. High-pressure noble gas jet injection is a mitigation technique which potentially satisfies the requirements of fast response time and reliability, without degrading subsequent discharges. Previously reported gas jet experiments on DIII-D showed good success at reducing deleterious disruption effects. In this paper, results of recent gas jet disruption mitigation experiments on Alcator C-Mod and DIII-D are reported. Jointly, these experiments have greatly improved the understanding of gas jet dynamics and the processes involved in mitigating disruption effects. In both machines, the sequence of events following gas injection is observed to be quite similar: the jet neutrals stop near the plasma edge, the edge temperature collapses, and large MHD modes are quickly destabilized, mixing the hot plasma core with the edge impurity ions and radiating away the plasma thermal energy. High radiated power fractions are achieved, thus reducing the conducted heat loads to the chamber walls and divertor. A significant (2× or more) reduction in halo current is also observed. Runaway electron generation is small or absent. These similar results in two quite different tokamaks are encouraging for the applicability of this disruption mitigation technique to ITER.

1. Introduction

Disruptions are a major concern for tokamaks, not just for present-day machines, but even more so for ITER and future tokamak reactors. Damage can arise from several different effects, including electromagnetic loads on conducting structures due to halo and induced currents, sudden thermal loads on divertor surfaces, and impact of disruption-generated relativistic electrons. Reliable mitigation of these problems using benign, robust techniques would be a key improvement in tokamak operation. High pressure noble gas jet injection (aka massive gas injection, or MGI) can potentially mitigate all three of these effects, while also satisfying the operational requirements of fast response time, robustness, and reliability, without impacting subsequent discharges.

Previously reported MGI experiments on the DIII-D tokamak[1] have shown good success at reducing the deleterious effects of disruptions. But the physics of the gas jet penetration and disruption mitigation was not understood well enough to reliably extrapolate the effectiveness of this approach to ITER-like plasmas, which are expected to have of order 1000× the stored energy of present-day machines. Experiments to address these questions have continued on DIII-D, which has $\beta_{\rm p}$ close to ITER, and have begun on Alcator C-Mod, which can reach plasma pressures and energy densities representative of ITER. On both machines, gas jet penetration, MHD behavior, and dependence on gas species is found to be remarkably similar.

2. Mitigation of Disruption Effects

Mitigation of both halo currents and divertor thermal deposition ultimately depends on the ability to convert a significant fraction of the total plasma stored energy, $W_{\rm tot} = W_{\rm th} + W_{\rm mag}$, into benign radiation on a timescale faster than an unmitigated disruption. Motivated by the earlier DIII-D results, an optimised high-pressure gas jet system has now been installed on C-Mod and experiments have been carried out to study the viability of this mitigation technique as parameters are pushed to more ITER-like plasma conditions. For the C-Mod plasmas used in the initial gas jet experiments described here, $W_{\rm tot} \simeq 0.75$ MJ, and the disruption timescale is ≤ 5 ms. Thus the impurities introduced by the gas jet have to radiate at a power level of order 0.1-1 GW for 1-2 ms. Therefore C-Mod provides a very challenging test of the ability to convert stored energy into radiation, in addition to the gas jet/impurity penetration issue.

2.1. Mitigation of Halo Currents

It has been found empirically that if a disrupting plasma is terminated quickly enough, halo currents in the divertor region are reduced[2]. Since the current quench time is determined by the L/R time of the post-thermal quench plasma, the current quench can be hastened if the resistivity is significantly increased, which is accomplished by decreasing the temperature of the post-thermal quench plasma and/or increasing $Z_{\rm eff}$. Noble gas jet injection on C-Mod and DIII-D has been shown to be an effective means of reducing the plasma temperature and initiating the disruption current quench[3, 4]. However, for successful halo current mitigation, the plasma resistivity must be kept high for the entire duration of the current quench. Even though most of the initial plasma thermal energy, $W_{\rm th}$, is eliminated from the plasma at the thermal quench, there still remains a large reservoir of energy stored in the poloidal magnetic field associated with the plasma current: $W_{\rm mag} = \frac{1}{2} L I_{\rm p}^2$. Here L is the plasma inductance, $L = \mu_0 R \left[\ell_{\rm i}/2 + \ln\left(8R/a\right) - 2\right]$, and $\ell_{\rm i}$ is the dimensionless internal inductance. During the current quench this energy is dissipated as Joule heating of the plasma and conducting structures. In C-Mod, $W_{\rm mag}$ greatly dominates the energy stored in the pre-disruption plasma. In fact, in unmitigated disruptions on C-Mod, the magnetic energy released during the current quench typically reheats the plasma to several hundred eV, resulting in an overall current quench time of ~ 4 ms, as shown in Figure 1a. This is enough time for the vertical displacement to carry the plasma all the way down to the divertor structure, leading to high electromagnetic and thermal loads there. In order to successfully speed up the current quench, the gas jet impurities have to be capable of continuing to radiate away the magnetic energy as it is dissipated throughout the entire current quench so that the plasma stays cold (i.e. short L/R time). Figure 1b shows the same signals for a disruption with argon gas jet mitigation. The argon significantly increases the radiative loss of the magnetic energy, resulting in a colder

quenching plasma. This, in addition to the higher $Z_{\rm eff}$, gives a higher resistivity, and therefore a faster current quench (< 2 ms). Less time is available for the plasma to move vertically (10 vs 30 cm), and the total halo current is reduced by about 50%. It should be noted in Fig. 1 that even though the current quench time is significantly shorter in the mitigated case, the maximum dI_p/dt is similar, and therefore the induced eddy currents and resulting forces are not exacerbated by the gas jet mitigation.

The reduction in halo current is also seen for the other noble gases that have been used, as shown in Fig. 2. It can be seen that the mitigation of halo currents generally improves with the Z of the noble gas due to better radiating efficiencies and higher $Z_{\rm eff}$. This trend is also consistent with experiments and modeling done on DIII-D[5]. Measurements of the toroidal distribution of halo currents in DIII-D have also shown a 50% reduction in the toroidal asymmetry, so the mitigation of peak $\boldsymbol{J} \times \boldsymbol{B}$ loads due to halo currents may be even more.

2.2. Mitigation of Thermal Deposition to Divertor Surfaces

In addition to reducing halo currents, another goal of gas jet injection is to decrease the sudden thermal deposition on divertor strike surfaces that occurs during disruptions. In ITER and future reactors, this conducted heat flux is high enough to melt or vaporize significant quantities of divertor material. In common with halo current mitigation, the basic concept is to convert a large fraction of the total plasma energy, $W_{\rm th} + W_{\rm mag}$, into UV and visible radiation, which is isotropically emitted. This effectively disperses much of the plasma energy benignly over the relatively large surface area of the chamber walls, rather than having it conduct down the scrape-off to concentrate onto a relatively small strike area on the divertor. The greater the fraction of plasma energy that can be radiated away, the less will be available to heat the divertor strike surfaces.

As described in the previous section, it is clear that the higher-Z gases radiate sufficiently well to affect the energy balance on the timescale of the disruption. The total radiated power in C-Mod is measured with a foil bolometer having a wide-angle view of the plasma. This radiated energy, divided by the total initial plasma energy, gives the fraction radiated. The results for the different noble gases are shown in Figure 3. Not surprisingly, the radiated energy fraction increases to very high levels with the higher-Z gases. For comparison, unmitigated disruptions with similar plasma parameters have radiated energy fractions of 20-30%. Fig. 3 also further illustrates the relatively good reproducibility of the gas jet shots.

Given that the higher-Z gas jets convert most of the plasma energy into benign radiation, the remaining thermal energy that does conduct down to the divertor should be reduced, resulting in less heating of the divertor strike surfaces. This has been explicitly confirmed with infrared imaging of the outboard divertor surface. The IR-derived temperature as a function of time is shown in Figure 4 for three different gases, as well as an unmitigated disruption. It is seen that the helium gas jet reduces the divertor surface temperature compared to an unmitigated disruption, and the higher-Z gas jet cases are even better at mitigating the thermal deposition and heating of the divertor surface. These IR data confirm that the plasma stored energy is effectively converted into benign radiation by the gas jet impurities.

3. Gas jet delivery and penetration

High-speed imaging of the gas jet plumes on both DIII-D and C-Mod clearly show that the jet does not penetrate deeply into the plasma. On DIII-D this is true even when the ram pressure is greater than the plasma pressure and ablation pressure (Fig. 5).

These data are consistent with a theoretical picture that the toroidal field pressure ($B^2/2\mu_0$), which greatly surpasses the jet ram pressure, provides the stopping mechanism for the neutral jet[6]. Yet, despite only shallow penetration into the plasma edge, gas jet mitigation is seen to be very effective in both devices. This bodes well for ITER, since deep gas jet penetration will not be feasible on that machine. These results imply that the gas jet nozzle design and precise aiming are not actually important. This was confirmed by trying two different jet geometries on DIII-D: an 'open' jet with a 15 cm diameter aperture aimed at the top of the plasma, and a 'directed' jet with a 1.5 cm diameter aperture aimed at the magnetic axis, both with similar neutral gas delivery rates. The resulting shutdown time scales were found to be quite comparable for similar target discharges. The onset times of the thermal and current quenches, and the duration of the current quench were quite similar.

Another important result is that with present high-pressure gas jet systems, only a small fraction of the supplied gas actually gets into the vacuum chamber on the timescale of the disruption. For example, using a 15 ms long valve opening injecting a total of 5×10^{22} argon atoms, measurements of the jet outlet pressure in DIII-D indicate that only $\sim 10\%$ of the injected argon atoms arrive in the vessel prior to the start of the current quench (Fig. 6a), and only half of the argon actually arrives before the current quench is over. These findings have important implications on the efficacy of collisional suppression of runaway avalanching (see section 4).

3.1. Role of MHD

In order to understand how the shallow gas jet penetration observed in DIII-D and C-Mod can still result in effective disruption mitigation, detailed measurements of gas flow, impurity concentrations, T_e and n_e profile evolution, MHD activity, etcetera have been made in both machines, and extensive modeling of C-Mod equilibria with the NIMROD[7] 3-D MHD code has been carried out[8]. Since both the C-Mod and DIII-D equilibria had very similar q-profiles in these gas jet experiments ($q_{95} = 3.3 - 3.6$, $q_0 \approx 1.0$, monotonic), the MHD behavior should be similar on the two machines, and probably on ITER as well, at least in its baseline scenario ($q_{95} = 3.1$). And indeed, the experimental sequence of events, shown in Fig. 6 for DIII-D, qualitatively agrees with the NIMROD results from C-Mod. The edge temperature collapses when the gas jet contacts the plasma surface. This cold edge is used as the starting condition for the NIMROD simulations. A cooling front begins to propagate into the plasma, and when it reaches the $q = 2$ radius, the growth of an $m = 2/n = 1$ is triggered. This is observed experimentally (Fig. 6d,e) and seen in the NIMROD evolution (Fig. 7a). (For the modeling work described here, the NIMROD code did not yet have impurity transport or radiation included. The cooling front in the NIMROD result is due to the growth of MHD instabilities and destruction of closed flux surfaces, and its calculated effect on plasma energy transport.) T_e continues to rapidly collapse in to the $q = 1$ radius, leading to a large $m = 1/n = 1$ mode (Figs. 6f and 7b). This results in large ergodic regions and destruction of flux surfaces (Fig. 7c,d), loss of core confinement, mixing of impurities, and eventually triggering the current quench (Fig. 6g).

Additional evidence for the role of MHD on the impurity transport comes from DIII-D experiments where the radial depth of the $q = 2$ surface was varied[9]. The delay time until the start of the core thermal quench was found to increase with the distance of the $q = 2$ surface from the plasma edge, consistent with the picture that the cold front must propagate to the $q = 2$ surface to destabilize the 2/1 mode.

3.2. Gas species, mixed gases

There is a several millisecond delay between firing the fast high-pressure valve[10] and the appearance of the gas at the plasma surface. This transit time is limited by the sound speed of the gas through the delivery system. As mentioned previously, low-Z gases such as helium, which has a fast thermal speed, are not particularly good at disruption mitigation in C-Mod. Higher-Z gases, on the other hand, mitigate well, but have slower thermal speeds. However, experiments have been done on both machines using a mixture of a light gas (He on C-Mod, H_2 on DIII-D) with small amounts of argon. Since the high-pressure gas in the delivery system is in the viscous flow regime, the lighter gas carries the entrained argon along at its faster thermal velocity, thereby reducing the time delay between the firing of the jet and cooling of the plasma edge. This improvement in response time can be important when the gas jet is used to mitigate real, unplanned disruptions, particularly if the disruption timescale is short. An example of the improved response time is shown in Fig. 8 for a 98% H_2/ 2% Ar case in DIII-D. In this case, the improvement is seen to be about 2 ms, which is a 25% reduction in the delay time. It is also seen that the electron density reaches a higher value in the 98% H_2 case, indicating that argon impurity transport is slower than hydrogen.

4. Runaway electron suppression

Runaway electrons are not observed in the gas jet experiments on C-Mod, and only small runaway currents ($< 5\%$ of I_p) are seen occasionally on DIII-D gas jet shots. (The general lack of observed runaways is also true for unmitigated disruptions on both machines.) However, the number of electrons (free + bound) injected by the gas jet prior to the current quench is estimated to be insufficient to collisionally suppress runaway avalanching[11]. Figure 9 shows ideal (0-D) estimates of the delivered number of Ar atoms, N_{Ar} (obtained by integrating the jet pressure measured as a function of time and normalizing to the known steady-state flow rate), and number of free electrons, ΔN_e (measured with CO_2 interferometers) created in the plasma by the start of the current quench. Also shown is the estimated total (free + bound) electron number, N_{crit}, necessary for avalanche suppression at the start of the current quench; this is estimated from the plasma inductance and current decay rate. While the total electron number (free + bound) in the plasma is not measured directly, an estimate of this quantity can be made from the available data. A 'best case' value is given by $18N_{Ar}$, i.e. we assume that every argon injected by the gas jet is assimilated into the plasma. A more realistic value, however, is probably obtained if we take into account that the current quench plasma decay time, $\tau_{CQ} \approx 3 - 6$ ms, implies an electron temperature $T_e \approx 2 - 5$ eV, and mean charge state $Z_{eff} \approx 1 - 2$. Assuming $Z_{eff} = 1$, the total electron number in the plasma is approximately $18\Delta N_e$, shown in Fig. 9 by the dashed magenta line. It can be seen that the delivered electron number is, at best, $3 - 10\times$ (more realistically, $10 - 100\times$) too low to collisionally suppress the runaway electron avalanche, even in this ideal 0-D approximation.

Therefore the present experiments do not necessarily imply successful avoidance of runaway avalanching *via collisional suppression* in ITER. The lack of significant runaways in current C-Mod and DIII-D gas jet experiments may instead be due to some other physics, such as MHD destruction of magnetic flux surfaces[12]. This would be consistent with the large ergodic regions seen in the NIMROD modeling (Fig. 7c,d).

5. Summary

High-pressure noble gas injection has been shown to be a reliable, safe method for rapidly shutting down discharges in Alcator C-Mod and DIII-D tokamaks. In both machines, the sequence of events following gas injection is observed to be quite similar: the jet neutrals stop near the plasma edge, the edge temperature collapses, and large MHD modes are quickly destabilized, mixing the hot plasma core with the edge impurity ions and radiating away the plasma thermal energy. The details of jet aiming are not found to be important; rather, jet species and the neutral delivery rate to the plasma edge are found to be the crucial jet parameters for determining the resulting shutdown timescales. During the core thermal quench, high radiated power fractions are achieved, indicating a reduction of localized, conducted heat loads to the chamber walls and divertor when compared with normal, unmitigated disruptions. The strong thermal quench radiation results in a cold ($T_e \sim$ several eV) plasma in which the plasma current quickly decays resistively. During the current quench, a significant ($2\times$ or more) reduction in halo current forces is observed relative to normal disruptions. Also, runaway electron generation appears to be small or absent (as it is in unmitigated disruptions). Present data and MHD modeling suggest that this could be due to the large MHD modes observed, not the result of collisional (impurity) suppression of runaway avalanching. These similar results in two quite different tokamaks are encouraging for the applicability of this technique to ITER for avoidance of wall damage during disruptions. Additional experimental and theoretical work is underway at both Alcator C-MOD and DIII-D to help further understand the physical processes occurring during high-pressure noble gas injection.

Acknowledgments

This work is support by Department of Energy Coop. Agreements DE-FC02-99ER54512 and DE-FC02-04ER54698, Grants DE-FG02-04ER54758 and DE-FG02-04ER54762, and Contracts DE-AC05-00OR22725, W-7405-ENG-48, and W-7405-ENG-36.

References

[1] D.G. Whyte *et al*, Phys. Rev. Lett. **89** (2002) 055001.
[2] P.L. Taylor, A.G. Kellman, T.E. Evans, D.S. Gray, D.A. Humphreys A.W. Hyatt, T.C. Jernigan, R.L. Lee, J.A. Leuer, S.C. Luckhardt, P.B. Parks, M.J. Schaffer, D.G. Whyte, J. Zhang, Phys. of Plasmas **6** (1999) 1872-9.
[3] R.S. Granetz *et al*, Nucl. Fusion **46** (2006) 1001-8.
[4] D.G. Whyte, *et al*, J. Nucl. Mater **313** (2003) 1239.
[5] E. Hollmann, *et al*, Nucl. Fusion **45** (2005) 1046.
[6] P. Parks, General Atomics, private communication (2006).
[7] C.R. Sovinec, *et al*, J. Comput. Phys. **195** (2004) 355.
[8] V.A. Izzo, Nucl. Fusion **46** (2006) 541.
[9] E. Hollmann, *et al*, Phys. Plasmas **14** (2007) 12502-1-8.
[10] S.L. Milora, S.K. Combs, C.R. Foust, Rev. of Sci. Instrum. **57**, (1986) 2356-8.
[11] P. Parks, *et al*, Phys. Plasmas **7** (1999) 2523.
[12] R. Yoshino and S. Tokuda, Nucl. Fusion **40** (2000) 1293-1309.

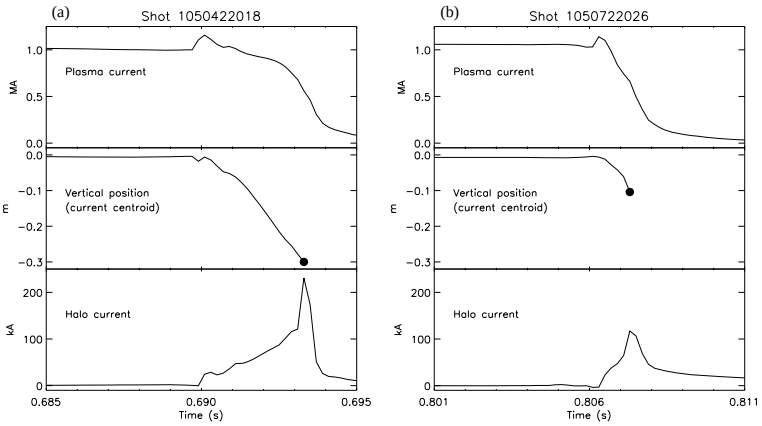

Figure 1. *Comparison of an unmitigated current quench (left) with an argon gas jet case (right) in C-Mod. The argon significantly shortens the current quench, resulting in much less vertical displacement and half the halo current. (The dot at the end of the displacement signal indicates the last time for which closed flux surfaces exist.)*

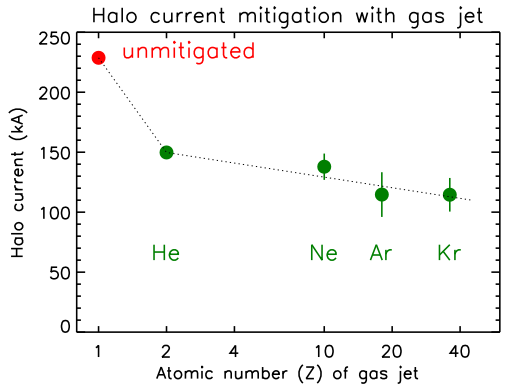

Figure 2. *Gas jet injection is effective at reducing halo currents in Alcator C-Mod when compared to unmitigated disruptions. Mitigation improves with the Z of the gas.*

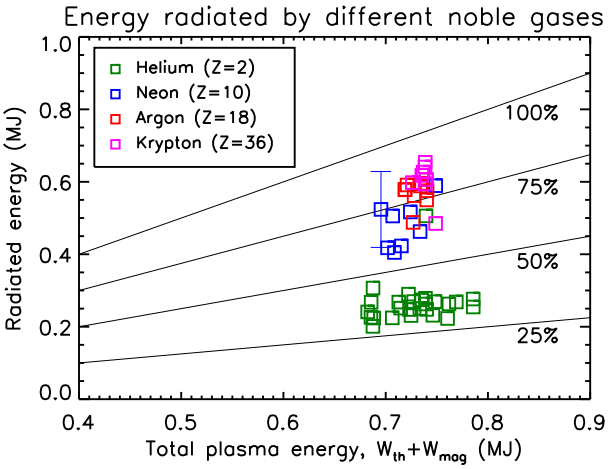

Figure 3. *The higher-Z gas jets convert most of the plasma energy in C-Mod into benign radiation. For comparison, unmitigated disruptions with similar plasma parameters have radiated energy fractions of 20-30%*

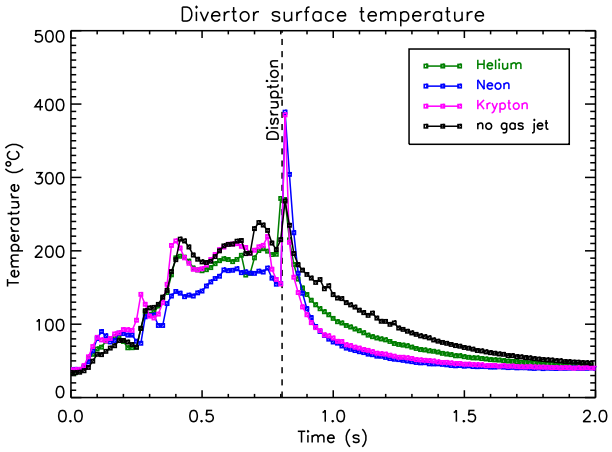

Figure 4. *IR-derived temperature of the divertor surface during several different gas jet disruptions in C-Mod. Gas jet injection reduces the temperature increase of the surface compared to unmitigated disruptions. Higher Z gases do better than low Z. (Note: disruption-induced shaking of the IR camera renders the first 60-70 ms of data after the disruption quantitatively inaccurate, therefore the amplitudes of the thermal spikes immediately after the disruption are not reliable.)*

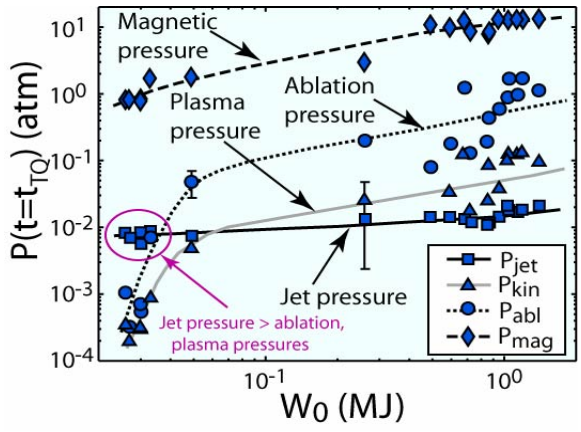

Figure 5. *Estimates of jet pressure, plasma pressure, ablation pressure on jet, and magnetic pressure in DIII-D, all at the thermal quench time at the radius of the jet stopping for different target plasma thermal energies, W_0.*

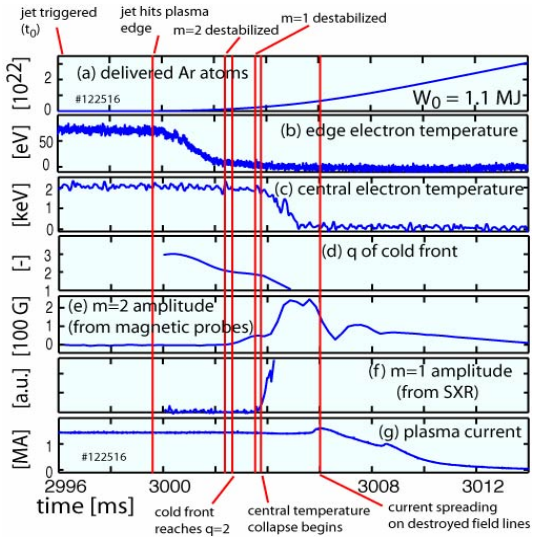

Figure 6. *Measurements of (a) delivered Ar neutrals, (b) edge electron temperature, (c) central electron temperature, (d) local q at the cold front, (e) $m = 2$ amplitude of poloidal magnetic field perturbations, (f) $m = 1$ amplitude, and (g) plasma current as a function of time for an argon gas jet shot in DIII-D.*

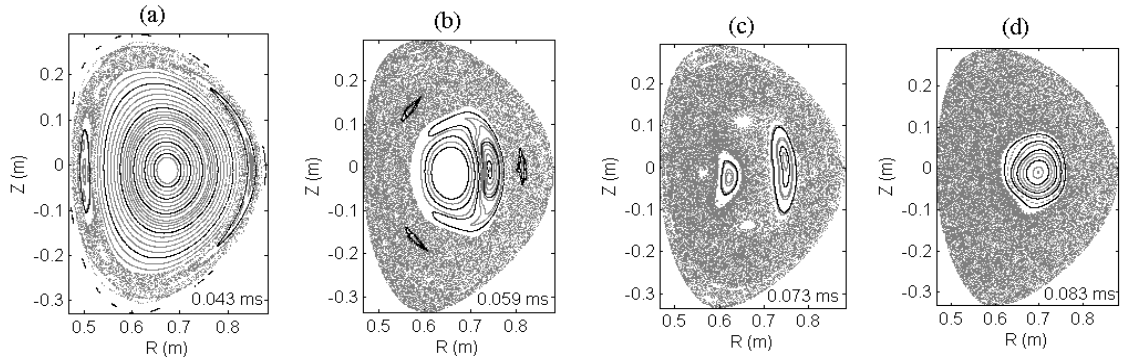

Figure 7. *Modeling of C-Mod equilibrium with NIMROD predicts fast growing 2/1 and 1/1 MHD tearing modes which result in ergodic field lines over much of the plasma cross-section and loss of confinement. The NIMROD timescale shown is a factor of ∼20 faster than in the actual experiment due to the lower Lundquist number used in the modeling.*

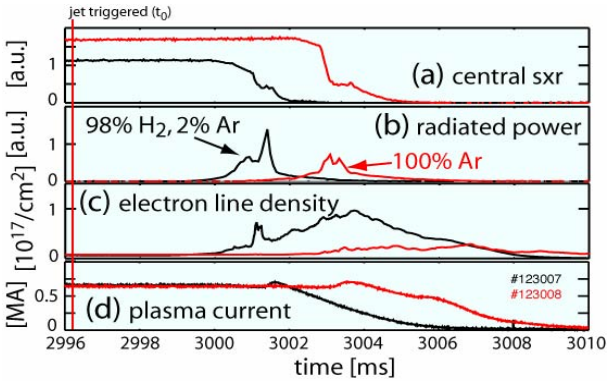

Figure 8. *Comparison of shutdown timescales for 100% Ar vs 98% H_2/ 2% Ar gas jet injection in DIII-D, showing (a) central soft x-ray (proxy for $T_e(0)$), (b) radiated power, (c) electron line density, and (d) plasma current as a function of time.*

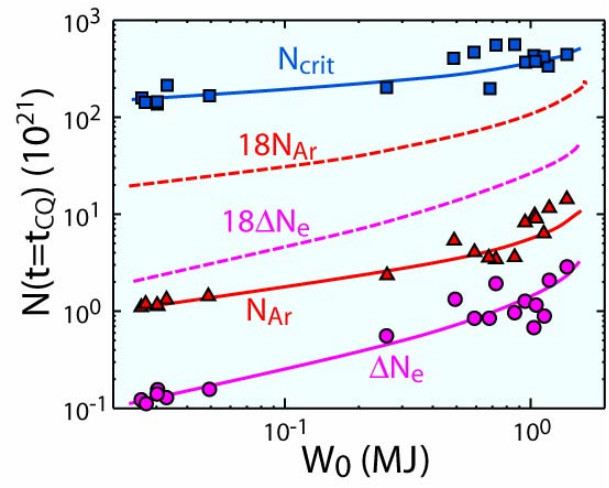

Figure 9. *Measured free electron increase, ΔN_e, and number of delivered argon atoms, N_{Ar}, at the current quench onset, and estimated electron number, N_{crit}, necessary for runaway electron suppression; all as a function of initial plasma thermal energy, W_0, in DIII-D. The quantities $18N_{Ar}$ and $18\Delta N_e$ are different estimates of the total number of electrons (free + bound) added to the plasma by the argon injection, and are explained in more detail in the text.*